UNIVERSITÉ DE GENÈVE

Archive ouverte UNIGE
https://archive-ouverte.unige.ch

Article scientifique | Article | 2007

Published version | Open Access

This is the published version of the publication, made available in accordance with the publisher's policy.

Model-based analysis of Gd-BOPTA-induced MR signal intensity changes in cirrhotic rat livers

Planchamp Messeiller, Corinne; Gex-Fabry, Marianne; Becker, Christoph; Pastor, Catherine

How to cite

PLANCHAMP MESSEILLER, Corinne et al. Model-based analysis of Gd-BOPTA-induced MR signal intensity changes in cirrhotic rat livers. In: Investigative radiology, 2007, vol. 42, n° 7, p. 513–521. doi: 10.1097/RLI.0b013e318036b450

This publication URL: https://archive-ouverte.unige.ch/unige:42523
Publication DOI: 10.1097/RLI.0b013e318036b450

© This document is protected by copyright. Please refer to copyright holder(s) for terms of use.

Model-Based Analysis of Gd-BOPTA-Induced MR Signal Intensity Changes in Cirrhotic Rat Livers

Corinne Planchamp, PhD, Marianne Gex-Fabry, PhD,† Christoph D. Becker, MD,‡ and Catherine M. Pastor, MD, PhD**

Objective: To quantify the hepatic transport of the hepatobiliary contrast agent gadobenate dimeglumine (Gd-BOPTA) in rats with biliary cirrhosis of various severity degrees from magnetic resonance (MR) signal intensities using a population pharmacokinetic approach.

Materials and Methods: MR signal intensity was recorded during the Gd-BOPTA perfusion of normal and cirrhotic isolated rat livers. Similar experiments were conducted with ^{153}Gd-labeled Gd-BOPTA to quantify Gd-BOPTA content in liver, bile, and perfusate. All experimental data were analyzed together according to a population pharmacokinetic approach.

Results: A 6-compartment model developed from the radioactivity data adequately fit all MRI data when 4 image parameters were added to describe the relationship between the amount of contrast agent and the signal intensity. The model showed that entry of Gd-BOPTA into hepatocytes was decreased in cirrhotic livers when compared to normal livers.

Conclusions: Although the MR signal intensity is similar in normal and cirrhotic livers, the population pharmacokinetic approach developed in this study shows a decreased entry of Gd-BOPTA into cirrhotic hepatocytes.

Key Words: MRI, contrast agent, Gd-BOPTA, population pharmacokinetic modeling, liver cirrhosis

(*Invest Radiol* 2007;42: 513–521)

Gadobenate dimeglumine (Gd-BOPTA) is a hepatobiliary magnetic resonance imaging (MRI) contrast agent similar to the extracellular contrast agent gadopentetate dimeglumine (Gd-DTPA), but with a lipophilic moiety that enables uptake by hepatocytes and excretion into bile. Thus, in addition to the detection of hypervascular lesions in the postinjection phase similar to other extracellular contrast agents, it may improve the characterization of hepatic lesions in the delayed hepatobiliary phase.[1–5] Gd-BOPTA enters into rat hepatocytes through a transporter belonging to the organic anion transporting polypeptide family (Oatps)[6–8] and is excreted unchanged into bile through the ATP-dependent multidrug resistance-associated protein 2 (Mrp2).[9–12]

In cirrhosis induced by a chronic bile duct ligation (BDL), the expression of rat $Oatp_1$, $Oatp_2$, and Mrp_2 is down-regulated.[13,14] In this model, we previously observed that the decreased expression of hepatic transporters was not associated with changes in Gd-BOPTA-induced signal intensity enhancement.[14] The MR signal intensity was similar during Gd-BOPTA perfusion in mild cirrhotic and normal livers. We then hypothesized that the concomitant diminution in uptake and biliary excretion of Gd-BOPTA might result in a sustained concentration within cirrhotic hepatocytes.

We previously quantified Gd-BOPTA uptake and biliary excretion from dynamic MRI in normal rat livers with a compartmental pharmacokinetic model validated with ^{153}Gd-BOPTA.[15] A 6-compartment, 8-rate constants open model was considered to describe the pharmacokinetics of ^{153}Gd-labeled Gd-BOPTA. Because perfusate and bile data were not available in MRI experiments, a reduced form of the model (6-compartment, 5-rate constants) was considered for the MRI data. This was the first pharmacokinetic analysis of MR signal intensities reported with a hepatobiliary contrast agent that enters into hepatocytes and is eliminated by bile.

In the present study, we extended the pharmacokinetic analysis of Gd-BOPTA hepatic transport in perfused livers isolated from rats with biliary cirrhosis of various severity degrees. Data obtained from normal and cirrhotic rats with radioactivity and MRI detection were analyzed together according to an approach of population pharmacokinetics.[16] With this approach, each experiment contributes to estimate mean population parameters and variabilities of these parameters, whereas parameter estimates for each experiment gain from knowledge accumulated from the entire population. Population pharmacokinetics is often used during drug development to evaluate the source of interindividual variability on the basis of sparse data in large patient populations. In the MRI field, it has recently been used to assess Gd-DTPA kinetics in tumors.[17,18] Here, this approach allowed us to analyze MRI experiments together with radioactivity exper-

Received November 2, 2006, and accepted for publication, after revision, January 13, 2007.

From the *Laboratoire de Physiopathologie Hépatique et Imagerie Moléculaire; and Département de †Psychiatrie, ‡Radiologie, Hôpitaux Universitaires de Genève, Geneva, Switzerland.

Supported by the "Fonds National Suisse de la Recherche Scientifique" N° 3200-109977 (to C.M. Pastor).

Reprints: Catherine M. Pastor, MD, PhD, Hôpitaux Universitaires de Genève, Laboratoire de Physiopathologie Hépatique et Imagerie Moléculaire, Rue Micheli-du-Crest, 24, 1205 Geneva, Switzerland. E-mail: catherine.pastor@hcuge.ch.

Copyright © 2007 by Lippincott Williams & Wilkins

ISSN: 0020-9996/07/0007-0513

Copyright © Lippincott Williams & Wilkins. Unauthorized reproduction of this article is prohibited.

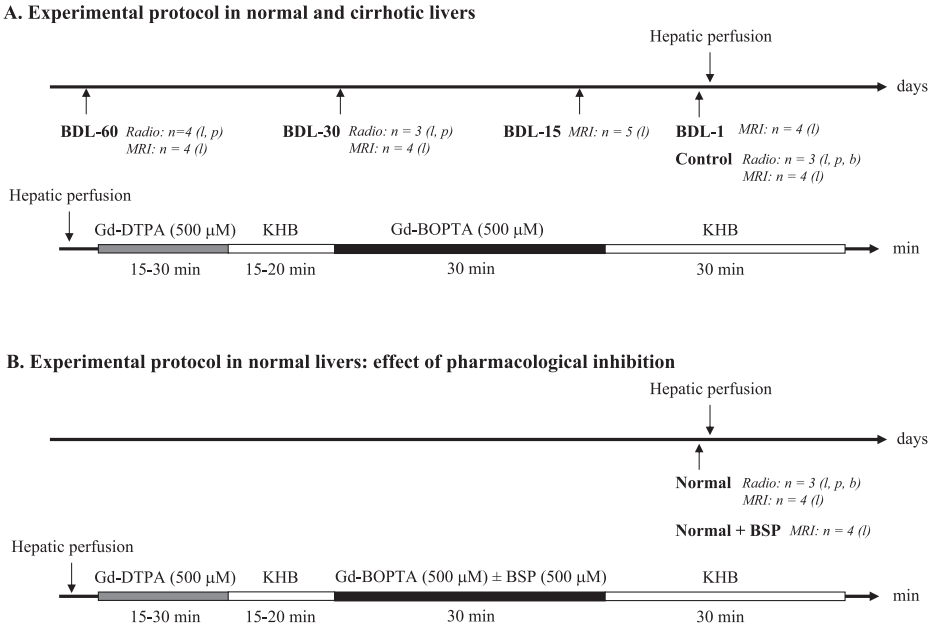

FIGURE 1. Experimental protocol in: (A) normal and cirrhotic livers; and (B) normal livers with pharmacological inhibition. Biliary cirrhosis was induced by bile duct ligation and livers were perfused 15 (BDL-15), 30 (BDL-30), and 60 (BDL-60) days later. An additional group of rats had BDL at the time of perfusion (BDL-1). Livers were perfused with either ^{153}Gd-labeled Gd-DTPA and ^{153}Gd-labeled Gd-BOPTA with radioactivity detection (radio) or with Gd-DTPA and Gd-BOPTA in the MRI room (MRI). Available samples are indicated in brackets (l = liver, p = perfusate, b = bile). In (B), normal livers rats were perfused with Gd-BOPTA ± bromosulfophthalein (BSP).

iments in normal and cirrhotic rats in a single model. Interpretation of MRI signal kinetics benefited from the more complete information obtained with radioactivity data. Finally, individual parameter estimates were analyzed to study Gd-BOPTA transport in cirrhotic rat livers.

MATERIALS AND METHODS

Chemicals

Gd-BOPTA (MultiHance, Bracco Imaging, Italy) and Gd-DTPA (Magnevist, Schering, Germany) are commercially available. $^{153}GdCl_3$ (1 GBq/mL) was obtained from Gamma-Service Isotopen und Strahlentechnik GmbH (Leipzig, Germany). All other chemicals were of analytical grade.

^{153}Gd-labeled Gd-DTPA and Gd-BOPTA were obtained by adding $^{153}GdCl_3$ (1 MBq/mL) to the commercially available 0.5 M solutions that contain a slight excess of ligand DTPA and BOPTA. Contrast agents were diluted in Krebs–Henseleit-bicarbonate (KHB) solution to obtain a 500 μM concentration in the perfusion solution.

Animals and Liver Perfusion

Before surgery for perfusion experiments, Sprague-Dawley rats (Charles River, l'Arbreste, France; 300–450 g) were anesthetized with pentobarbital (50 mg/kg intraperitoneal [IP]). The protocol was approved by the animal welfare committee of the University of Geneva and the veterinary office and followed guidelines for the care and use of laboratory animals.

Livers were perfused in situ as previously described.[15] To avoid liver injury, isolated livers were left in the dead rats (another possibility is to isolate and explant the organ). When livers were perfused in the Nuclear Medicine laboratory, the common bile duct was cannulated with a PE 10 catheter to collect bile samples (bile collection was impossible for experiments made with the MR scanner). During perfusion, the liver viability was assessed by monitoring portal vein pressure (Hewlett Packard 78353B, Palo Alto, CA). We previously showed that the portal pressure and the hepatic O_2 consumption remained constant during the perfusion of both contrast agents.[8]

Experimental Protocols

Biliary cirrhosis was induced by chronic ligation of the bile duct. After laparotomy (2–3% isoflurane anesthesia), rats had a double ligation of the common bile duct with section between the 2 ligatures. For MRI experiments, rats recovered from surgery and were perfused 15 (BDL-15, n = 5), 30 (BDL-30, n = 4), and 60 (BDL-60, n = 4) days later (Fig. 1A). An additional group of rats had BDL 1–2 hours before perfusion (BDL-1, n = 4) while 4 normal rats were perfused. To evidence the extracellular diffusion space, each liver was perfused with KHB solution + Gd-DTPA (500 μM), followed by KHB solution for washing. To study the hepatocyte entry of Gd-BOPTA (500 μM), the same liver was perfused with KHB solution + Gd-BOPTA, followed by KHB solution for washing. In each liver, Gd-DTPA was perfused before Gd-BOPTA. For radioactivity experiments, normal (n = 3) and BDL (n = 7) rats were perfused with ^{153}Gd-labeled Gd-DTPA (500 μM) and ^{153}Gd-labeled Gd-BOPTA (500 μM). In addition, we perfused normal livers with a solution containing Gd-BOPTA perfusion + bromosulfophthalein (500 μM), which is a pharmacological inhibitor of Oatps transporters (Fig. 1B).

Radioactivity Experiments

A gamma-scintillation probe with a lead collimator was placed 1 cm over the liver and radioactivity was measured continuously during the perfusion of ^{153}Gd-labeled Gd-DTPA (500 μM) and ^{153}Gd-labeled Gd-BOPTA (500 μM).[15] Bile and outflow perfusate samples were collected every 5 minutes, weighted, and the radioactivity was determined by a Packard Cobra Auto-Gamma counter (Canberra Packard,

© 2007 Lippincott Williams & Wilkins
Copyright © Lippincott Williams & Wilkins. Unauthorized reproduction of this article is prohibited.

Switzerland). At the end of each experiment, portal vein, thoracic inferior vena cava, and bile duct were clamped and the liver was removed, weighted, and radioactivity was measured with a dose calibrator (Isomed 2000, MED Nuklear-Medizintechnik, Germany). In each experiment, the amount of contrast agent perfused was totally recovered in perfusate, liver, and bile, confirming that each experiment was correctly conducted.

MRI Experiments

Perfused livers were inserted into a wrist coil.[15] MRI was performed on a 1.5 T Eclipse MR system (Philips Medical System, Cleveland, OH). An axial image was obtained using a fast-gradient echo T1 weighted MR sequence preceded by a 90° saturation pulse with the following parameters: inversion time, 29 milliseconds; repetition time, 6.8 milliseconds; echo time, 3 milliseconds; flip angle, 90°; matrix, 256 × 256; 1 image/8 seconds; field of view (FOV), 14 cm; and slice thickness, 7 mm. Mean signal intensity was measured in a region of interest drawn on the short axis view of the liver to encompass a hepatic lobe. The signal intensity measured during Gd-DTPA (500 μM) and Gd-BOPTA (500 μM) perfusion in the liver was normalized to muscle signal intensity. For each liver, the region of interest remained constant during the entire experiment, but could vary between livers.

Pharmacokinetic Modeling

Structural Pharmacokinetic Model

We previously showed that a 6-compartment 8-rate constants structural model adequately described the pharmacokinetics of ^{153}Gd-labeled Gd-DTPA and ^{153}Gd-labeled Gd-BOPTA in perfused livers isolated from normal rats.[15] As shown in Figure 2, compartments 2, 4, and 5 of the liver depict the amount of contrast agent in extracellular space $A_2(t)$, into hepatocytes $A_4(t)$, and into a secondary hepatocyte-associated space $A_5(t)$. Compartment 3 represents the amount of contrast agent in the outflow perfusate $A_3(t)$ and compartment 6 represents the amount in bile $A_6(t)$. Compartment 1, with amounts of contrast agent $[A_1(t)]$, reflects the in-homogeneity of the perfusion solution at the beginning and end of perfusion (solution of contrast agent mixing in the perfusion system or disappearing from the system). Entry of contrast agent into the system is modeled as a zero-order infusion rate k_{in} over a time period τ. First-order rate constants k_{ij} are defined with respect to the compartment of origin i and the compartment of convergence j. The amount versus time profiles of Gd-DTPA (D) and Gd-BOPTA (B) are modeled simultaneously. K_{12} and k_{23} of both contrast agents are identical because they share the same access to the system and extracellular space. Gd-DTPA enters into the cellular compartment 4 with a rate constant $k_{24}(D)$ postulated to be much smaller than the one of Gd-BOPTA, $k_{24}(B)$.

For radioactivity experiments, observed amounts in perfusate, bile, and liver were modeled as previously described,[15] with k_{46} and k_{56} (rate constants for the transfer of Gd-BOPTA from hepatocytes to bile) set to 0 for BDL experiments. For MRI experiments, the relationship between signal intensity and amount of contrast agent previously described[15] was modified to include the possibility of signal saturation in each compartment:

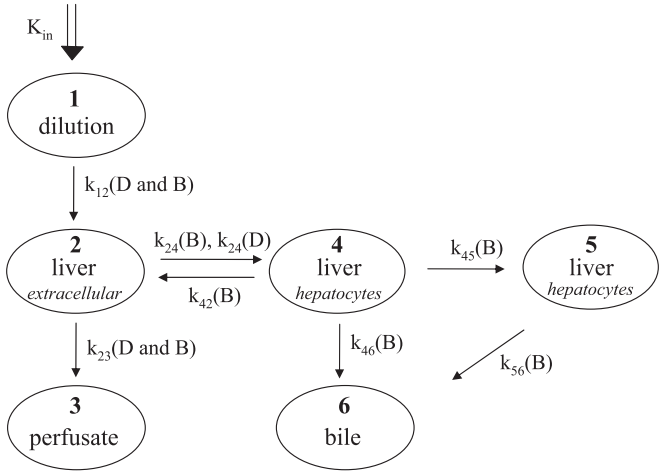

FIGURE 2. Pharmacokinetic model. Compartments 2, 4, and 5 of the liver depict the amount of contrast agent in extracellular space $A_2(t)$, into hepatocytes $A_4(t)$, and into a secondary hepatocyte-associated space $A_5(t)$. Compartment 3 represents the amount of contrast agent in the outflow perfusate $A_3(t)$ and compartment 6 represents the amount in bile $A_6(t)$. Compartment 1, with amounts of contrast agent $[A_1(t)]$, reflects the in-homogeneity of the perfusion solution at the beginning and end of perfusion (solution of contrast agent mixing in the perfusion system or disappearing from the system). Entry of contrast agent into the system is modeled as a zero-order infusion rate k_{in} over a time period τ. First-order rate constants k_{ij} are defined with respect to the compartment of origin i and the compartment of convergence j. The amount versus time profiles of Gd-DTPA (D) and Gd-BOPTA (B) are modeled simultaneously. K_{12} and k_{23} of both contrast agents are identical because they share the same access to the system and extracellular space. Gd-DTPA enters into cellular compartment 4 with a rate constant $k_{24}(D)$ postulated to be much smaller than the one of Gd-BOPTA $k_{24}(B)$.

$$SI(t)_{pred} = s_0 + g_2 \frac{A_2(t) \cdot ASAT_2}{A_2(t) + ASAT_2} + g_4 \frac{A_4(t) \cdot ASAT_4}{A_4(t) + ASAT_4} + g_5 \frac{A_5(t) \cdot ASAT_5}{A_5(t) + ASAT_5} \quad (1)$$

$SI(t)_{pred}$ is the model predicted average signal intensity in the region of interest in the liver; s_0 is baseline signal; g_2, g_4, and g_5 are tissue-specific constants of proportionality depending on native relaxation rate and relaxivity[17,19,20]; and $ASAT_2$, $ASAT_4$, and $ASAT_5$ are the amounts of contrast agent leading to half maximum signal enhancement for a given compartment.

Population Pharmacokinetic Model

The population pharmacokinetic model estimates the population average values of pharmacokinetic parameters, between-experiments variabilities of these parameters, as well as residual variability (discrepancy between model pre-

© 2007 Lippincott Williams & Wilkins

Copyright © Lippincott Williams & Wilkins. Unauthorized reproduction of this article is prohibited.

diction and observation).[21] An exponential model described between-experiments variabilities of parameters:

$$k_i = \bar{k} \cdot e^{\eta_i} \quad (2)$$

k_i is the estimate of any pharmacokinetic parameter for a given experiment, $\bar{k}$ represents the population mean estimate for the complete set of experiments, and η_i is the individual variation from this mean value. η_i are assumed to be normally distributed with mean 0 and variance ω^2. In addition to population values, individual parameters of the different experiments were obtained according to a Bayesian procedure.

Model Assessment

The structural pharmacokinetic model was described by a set of differential equations implemented in the NONMEM software (version V, University of California, San Francisco, CA) that can integrate data of different nature (amounts with radioactivity experiments and signal intensities with MRI), obtained from different perfused substances (Gd-DTPA and Gd-BOPTA), different types of samples (liver, perfusate, and bile), and from different populations (normal and cirrhotic rats), with missing data (no bile and perfusate with MRI).[22] Subroutines ADVAN6 and TRANS1 were used for model description. Parameters were estimated via a maximum likelihood approach, whereby an objective approach was minimized using first-order linearization (FO method).

In a first step, optimization of the population model was performed with the population of 10 normal and cirrhotic rats from radioactivity experiments. Variability was introduced step-by-step on each rate constants to obtain the best model (except for k_{12} that reflected a property of the experimental apparatus). Statistical comparison of models was based on a likelihood ratio test withdraw; that is, a χ^2 test of the difference of objective functions (the lower the value, the better the fit), with $P < 0.01$ considered to represent a significantly better fit.[15] When 2 models performed similarly, the simplest model was selected (principle of parsimony). In addition, standard errors of parameter estimates and correlations between them were considered. Graphical assessment of the goodness-of-fit was performed by displaying observed and predicted amounts of contrast agents or signal intensities at the population and individual levels.

In a second step, MRI data were added to the previous database, the rate constants, and variability terms being fixed to the values obtained with radioactivity data. Effort was first provided to optimize the relationship between signal intensity and amount of contrast agent [Eq. (1), proportionality and saturation constants]. Comparison of models proceeded as outlined for radioactivity experiments.

MRI data from livers coperfused with Gd-BOPTA + bromosulfophthalein were finally added to the database and analyzed with the best model identified in the previous stages.

Statistical Analysis

Data are given as median (minimum–maximum). Comparison between the experimental groups was performed with a Mann–Whitney *U* test (2 groups) or with a Kruskal–Wallis analysis and Dunn's multiple comparison test (>2 groups). $P < 0.05$ was considered significant.

RESULTS

Radioactivity Data

During the perfusion of 500 μM Gd-DTPA (total perfusion: 450 mL or 225 μmol) in normal livers, the hepatic amount of contrast agent rapidly increased toward steady state (1.5–1.7 μmol) and was completely washed out during the subsequent KHB perfusion (Fig. 3). No Gd-DTPA was excreted into bile. During the perfusion of 500 μM Gd-BOPTA (total perfusion: 900 mL, 450 μmol), the contrast agent amount in the liver increased up to 10–12 μmol. After washing of Gd-BOPTA with KHB solution, 1.7–2.8 μmol remained in the liver and 18–22 μmol were excreted into bile. In BDL livers, hepatic amount of Gd-DTPA increased to a higher amount (2.9–5.4 μmol in BDL-30 and 5.5–6.1 μmol in BDL-60) than in normal livers and was slowly washed out during KHB perfusion. During the perfusion of Gd-BOPTA, the hepatic accumulation was higher in cirrhotic than in normal livers (12–26 μmol in BDL-30 and 18–26 μmol in BDL-60). After washing of Gd-BOPTA with KHB solution, elevated amount of contrast agent (5–15 μmol in BDL-30 and 9–14 μmol in BDL-60) remained in the liver. No bile data was available because of bile duct ligation. Cumulative amount of Gd-BOPTA in perfusate at the end of experiment was slightly higher in BDL-30 (433–444 μmol) and BDL-60 (435–440 μmol) than in normal livers (426–428 μmol).

The pharmacokinetic modeling started from a model without between-experiments variability and proceeded with the step-by-step introduction of variability on the different rate constants, as summarized in Table 1. Variability terms were retained if they were associated with a significant decrease in the objective function and discarded if the objective function was not improved. The best population model (model f) was obtained with variabilities on the rate constant that describes the transfers: (1) from the extracellular space into the perfusate (k_{23} for Gd-DTPA and Gd-BOPTA, 43% variability); (2) from the extracellular space into hepatocytes (k_{24} for Gd-BOPTA, 67% variability); (3) from hepatocytes into perfusate (k_{42} for Gd-BOPTA, 18% variability); (4) from hepatocytes into bile (k_{46} for Gd-BOPTA, 21% variability); and (5) from perfusate into hepatocytes (tiny k_{24} for Gd-DTPA, 39% variability). This model perfectly fit all the radioactivity data (Fig. 3). The precision of all estimates was adequate with standard errors <20% on rate constants and <50% on variability.

MRI Data

For normal, BDL-1, BDL-15, and BDL-30 rats, the hepatic signal intensity increased toward a steady state (0.37–0.84 over baseline) during Gd-DTPA perfusion and rapidly returned to baseline value during the washout period (Fig. 4). However, the steady state was significantly higher in BDL-60 livers (0.71–0.85 over baseline, $P < 0.05$). The maximal signal intensity was much higher when livers were perfused with Gd-BOPTA (1.7–3.7) and in contrast to Gd-DTPA perfusion, the signal intensity did not return to baseline value

© 2007 Lippincott Williams & Wilkins

Copyright © Lippincott Williams & Wilkins. Unauthorized reproduction of this article is prohibited.

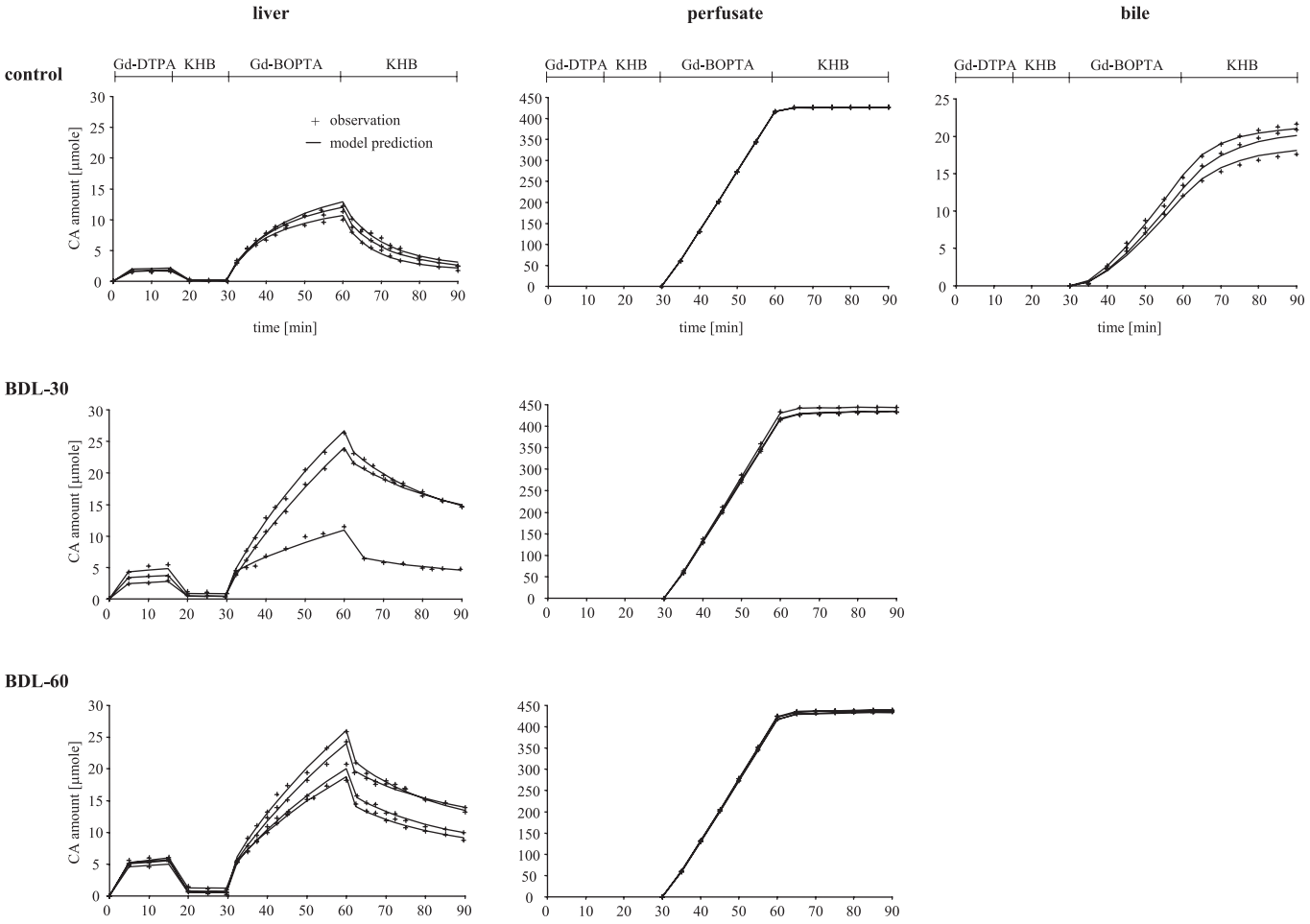

FIGURE 3. Radioactivity detection. Observed and model-predicted amount of contrast agent in liver, perfusate, and bile during the perfusion of 500 μM Gd-DTPA (15 minutes, 450 mL, 225 μmol), KHB solution (15 minutes), 500 μM Gd-BOPTA (30 minutes, 900 mL, 450 μmol), and KHB (30 minutes) in livers isolated from normal rats (n = 3), rats that had a bile duct ligation 30 days before hepatic perfusion (BDL-30, n = 3), and 60 days before perfusion (BDL-60 rats, n = 4). Predictions are calculated from the model shown in Figure 2, according to a population approach with post hoc estimation of parameters corresponding to individual experiments.

during the washout period. BDL-60 livers are different from the other groups, the maximal signal intensity during Gd-BOPTA perfusion being lower (1.2–1.3). This result contrasts with the radioactivity data of the same experimental group.

The MRI data (n = 21 experiments) were added to the radioactivity data in the NONMEM database and pharmacokinetic analysis was performed with model f (Table 1). The best fits were obtained when considering 4 image parameters for the relationship between the signal intensity and the amount of contrast agent [see Eq. (1)]. These parameters are 3 proportionality constants for each hepatic compartment (g_2, g_4, and g_5) and a unique signal saturation for the compartment 4 ($ASAT_4$) (Table 2, model iii). No variability was added on g_2, g_4, and g_5 because they reflect tissue-specific constants of proportionality depending on native relaxation rate and relaxivity, and consequently remain constant in all experimental groups.[18,22] $ASAT_4$ is a constant that depends on the MR sequence. Figure 4 shows the good performance of the model: (1) individual prediction overlaid the observed MRI data (Fig. 4A); (2) the distribution of values was randomly scattered around the unit line in the observed versus population-predicted signal intensity plot, and; (3) values were perfectly aligned on the unit line in the observed versus individual-predicted signal intensity plot (Fig. 4B). The precision of the proportionality constants was adequate with standard errors of the estimates $<$10% for g_2, $<$35% for g_4 and $ASAT_4$, and $<$70% for g_5.

Thus, the 6-compartment model developed from the radioactivity data adequately fit all MRI data when 4 image parameters were added to describe the relationship between amount of contrast agent and signal intensity. In normal livers, the model correctly predicted bile Gd-BOPTA accumulation from MRI data (9–20 μmol vs. 18–22 μmol from the radioactivity experiments), except for 1 experiment in which bile amount was most likely overestimated (59 μmol).

The individual estimates of rate constants from experimental groups in which both radioactivity and MRI experiments were available (normal, BDL-30, and BDL-60 groups)

© 2007 Lippincott Williams & Wilkins

Copyright © Lippincott Williams & Wilkins. Unauthorized reproduction of this article is prohibited.

TABLE 1. Development of the Population Model With the Radioactivity Data (n = 10 Experiments With 3 Control Rats, 3 Rats That had a Bile Duct Ligation 30 Days Before Hepatic Perfusion (BDL-30) and 4 Rats With a Bile Duct Ligation 60 Days Before Perfusion (BDL-60)

Model	(a)	(b)	(c)	(d)	(e)	(f)	(g)	(h)
Rate constants (min^{-1})								
k_{12}(D and B)	1.9	1.9	1.9	1.9	1.9	1.9	1.9	1.9
k_{23}(D and B)	4.7	5.1	4.7	4.7	4.6	4.7	4.7	4.7
k_{24}(B)	0.31	0.35	0.25	0.24	0.23	0.23	0.23	0.23
k_{42}(B)	0.031	0.045	0.028	0.035	0.035	0.027	0.028	0.028
k_{24}(D)	0.0089	0.013	0.011	0.011	0.011	0.011	0.011	0.011
k_{46}(B)	0.081	0.090	0.074	0.074	0.074	0.076	0.076	0.076
k_{45}(B)	0.013	0.026	0.015	0.016	0.016	0.014	0.015	0.015
k_{56}(B)	0.0072	0.014	0.013	0.015	0.016	0.013	0.014	0.013
Variability (%)								
k_{23}(D and B)	—	74	45	44	42	43	43	44
k_{24}(B)	—	—	65	66	63	67	66	68
k_{42}(B)	—	—	—	47	52	18	18	19
k_{24}(D)	—	—	—	—	36	39	37	37
k_{46}(B)	—	—	—	—	—	21	21	22
k_{45}(B)	—	—	—	—	—	—	0	0
k_{56}(B)	—	—	—	—	—	—	—	0
OF	1080	662	344	298	289	253	253	253
P	—	<0.001	<0.001	<0.001	<0.001	<0.01	NS	NS

Estimates corresponding to the best model (Model f) are highlighted.
K_{12}(D and B) was not investigated for variability because it reflects an intrinsic property of the experimental system.
D indicates Gd-DTPA; B, Gd-BOPTA; OF, objective function; $P < 0.01$, a significant improvement of fit; NS, nonsignificant improvement.

were compared according to the origin of the data (radioactivity vs. MRI) (Fig. 5). Values were largely similar for all rate constants, reinforcing the fact that data from both types of experiments can be analyzed together to study the effect of cirrhosis on the hepatic transport of Gd-BOPTA.

Effect of Cirrhosis on Gd-BOPTA Transport

The transfer rates k_{23} (from the extracellular space into the perfusate), k_{24} (Gd-BOPTA entry into hepatocytes), and k_{42} (efflux back of Gd-BOPTA from hepatocytes to the extracellular space) significantly differed between normal and cirrhotic livers (Fig. 5). The amount of contrast agent in the extracellular space increased with the severity of cirrhosis as indicated by the progressive diminution of k_{23} for Gd-DTPA and Gd-BOPTA in cirrhosis ($P = 0.0011$). The rate constant was significantly different in BDL-60 livers (3.7 $minutes^{-1}$) than in normal rats (7.9 $minutes^{-1}$). Entry of Gd-BOPTA into the main hepatic compartment (k_{24} for Gd-BOPTA) also significantly decreased in BDL-60 rats (0.089 $minutes^{-1}$ vs. 0.51 $minutes^{-1}$ in normal livers, $P < 0.005$). Gd-BOPTA efflux from hepatocytes back to the extracellular space differed across groups ($P < 0.005$). BDL-1 livers had a higher k_{42} (0.061 $minutes^{-1}$) than normal livers (0.022 $minutes^{-1}$), whereas values were close to normal in BDL-15, BDL-30, and BDL-60 livers (0.040, 0.031, and 0.030 $minutes^{-1}$, respectively). The unidirectional transfer rate of Gd-DTPA from the extracellular space into hepatocytes did not change between experimental groups and was 100 times lower than that observed with Gd-BOPTA. In normal livers, k_{24} for Gd-DTPA was 0.0065 $minutes^{-1}$, whereas k_{24} for Gd-BOPTA was 0.51 $minutes^{-1}$. Of note, k_{46} for Gd-BOPTA was irrelevant in BDL groups and was set to 0.

Effect of Pharmacological Inhibition With Bromosulfophthalein

The pharmacological inhibition of bromosulfophthalein on Gd-BOPTA entry into hepatocytes was studied in normal livers in the MRI room. During Gd-DTPA perfusion, MR signal intensity increased toward a steady state (0.3–0.5 over baseline) and rapidly returned to baseline value during the washout period (Fig. 6). A similar signal intensity versus time profile was observed during the perfusion of Gd-BOPTA + bromosulfophthalein.

Information from this group was added in the NONMEM database and analyzed with the model previously developed. Data were adequately fitted by the model (Fig. 6) and the pharmacokinetic modeling showed that Gd-BOPTA entry into hepatocytes was reduced 10 times by bromosulfophthalein (k_{24} was 0.046 $minutes^{-1}$ in Gd-BOPTA + bromosulfophthalein livers and 0.520 $minutes^{-1}$ in Gd-BOPTA livers).

DISCUSSION

In the present work, we developed a population pharmacokinetics approach to analyze MRI and radioactivity data obtained after the perfusion of normal and cirrhotic livers with MRI contrast agents. In a first stage, optimization of the pharmacokinetic model was performed with radioactivity experiments. Because experiments with radioactivity data

© 2007 Lippincott Williams & Wilkins
Copyright © Lippincott Williams & Wilkins. Unauthorized reproduction of this article is prohibited.

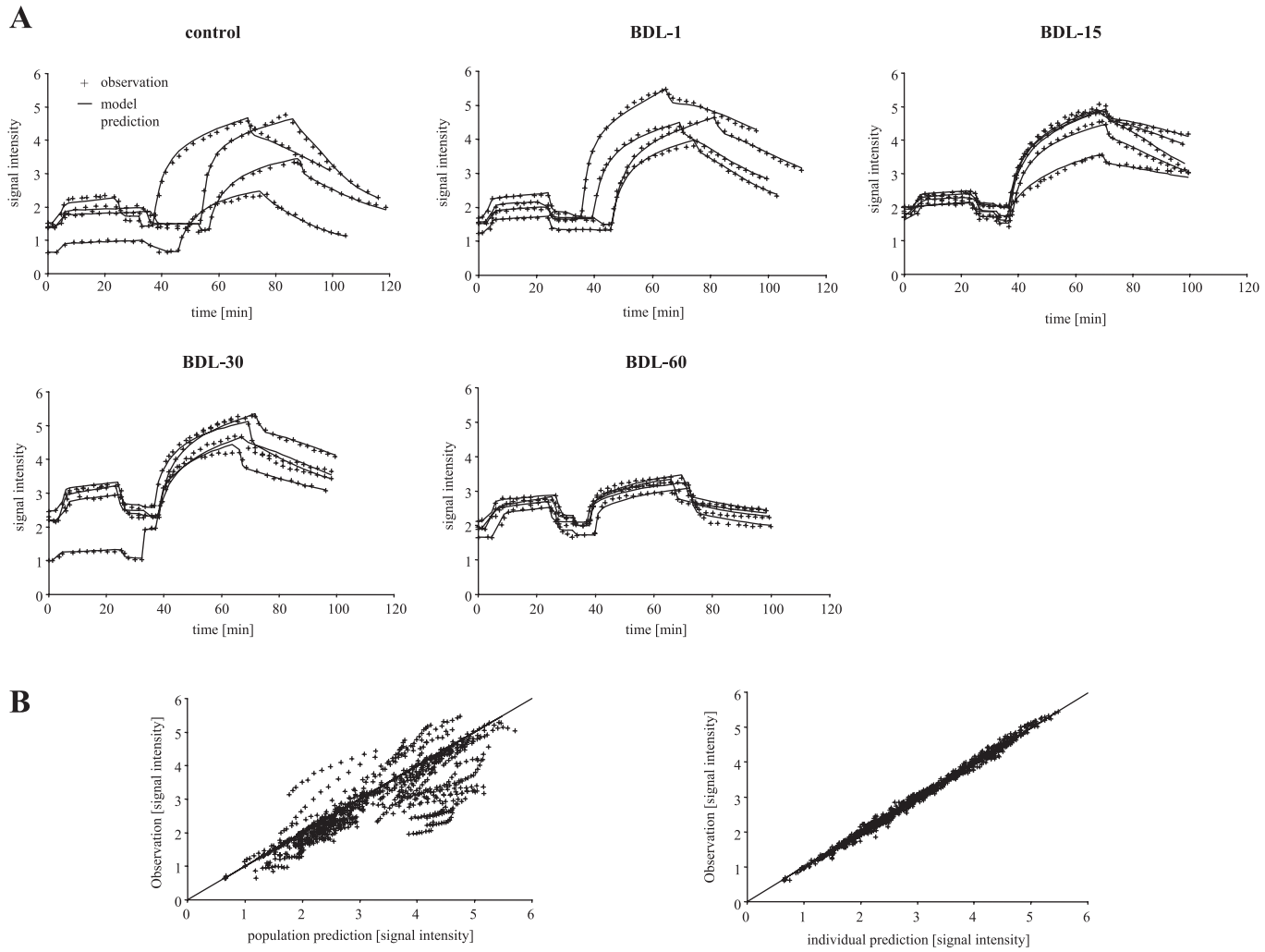

FIGURE 4. MRI detection. A, Observed and model-predicted signal intensity during the perfusion of Gd-DTPA (500 μM), KHB solution, Gd-BOPTA (500 μM), and KHB in livers isolated from normal rats (n = 4), from rats that had a bile duct ligation 1–2 hours before hepatic perfusion (BDL-1, n = 4), BDL-15 rats (n = 5), BDL-30 rats (n = 4), and BDL-60 rats (n = 4). Predictions are calculated from the model shown in Figure 2, according to a population approach with post hoc estimation of parameters corresponding to individual experiments. B, Observed versus model-predicted signal intensity at the level of the population (left) and the individual experiments (right). The continuous line is the unit line.

were fully controlled, they identified the major sources of between-experiments variability. By allowing the rate constants that describe major extra- and intracellular-associated processes to display variability, we successfully described the experiments performed in rats with different degrees of cirrhosis. The best model took into account variability on k_{23}(D and B), or transfer from the extracellular space into the perfusate on k_{24}(B), or Gd-BOPTA entry into hepatocytes k_{42}(B), or Gd-BOPTA efflux back to extracellular space and k_{46}(B), or Gd-BOPTA bile excretion. Variability also affected the rate constant describing the minor exchange of Gd-DTPA from the extracellular space into hepatocytes [k_{24}(D)].

In a second stage, the relationship between MRI signal and amounts of contrast agent in the liver compartments was analyzed. The proportionality constant relating signal intensity to contrast agent amount in hepatocytes (g_4) was higher than the one observed in the extracellular space (g_2) in accordance with higher relaxivity of Gd-BOPTA in protein-rich hepatocytes than in extracellular space filled with KHB solution.[23–27] Proportionality constant for the second hepatocyte-associated compartment (g_5) was small and difficult to estimate, as indicated by a large standard error. Although necessary to fit radioactivity data, this unidentified cell compartment might be of minor relevance for MRI images. Finally, goodness-of-fit improved when considering saturation of signal intensity with increasing amounts of contrast agent in hepatocytes. Indeed, radioactivity and MRI detection methods displayed qualitative differences in cirrhotic livers. Although hepatic Gd-BOPTA amount was higher in cirrhotic livers than in normal livers, according to radioactivity experiments, MR signal intensity was similar or diminished in

© 2007 Lippincott Williams & Wilkins

Copyright © Lippincott Williams & Wilkins. Unauthorized reproduction of this article is prohibited.

TABLE 2. Modeling of the Relationship Between Signal Intensity and Amount of Contrast Agent (n = 21 Experiments With 4 Control Rats, 4 Rats That Had a Bile Duct Ligation at the Time of Hepatic Perfusion [BDL-1], 5 BDL-15 rats, 4 BDL-30 rats, and 4 BDL-60 Rats)

Model	i	ii	iii	iv
Image parameters				
g_2	0.23	ND	0.16	0.15
g_4	0.38	ND	0.43	0.32
g_5	0.46	ND	0.11	0.18
$ASAT_2$	—	ND	—	—
$ASAT_4$	—	ND	7.3	12
$ASAT_5$	—	ND	—	2.5
OF	−1660	−1660	−2380	−2525
P	—	NS	<0.001	<0.001

Estimates corresponding to the best model (Model iii) are highlighted. Although Model iv was statistically better than Model iii, it was not identified as the best model because individual fits were unsatisfactory.

$P < 0.01$ indicates a significant improvement of fit; NS, nonsignificant; ND, not determined because calculation could not terminate; OF, objective function.

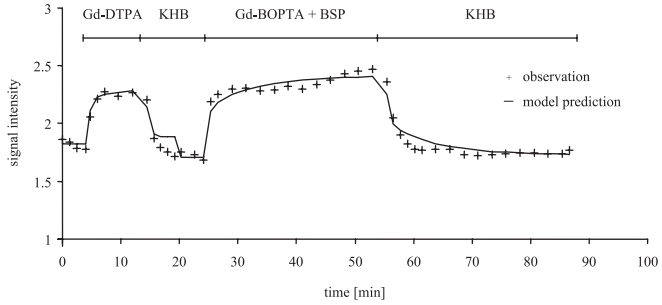

FIGURE 6. Observed and model-predicted signal intensity during the perfusion of Gd-DTPA, KHB solution, Gd-BOPTA + bromosulfophthalein, and KHB in livers isolated from normal rats (n = 4). For clarity, the result of a single experiment was shown but the results of the other experiments were similar.

cirrhosis. Because radioactivity experiments assess the exact amount of contrast agent in the liver, distortion of the signal intensity with the MR sequence used was the most likely explanation. For MRI experiments, we chose a fast-gradient echo T1 weighted MR sequence because it has a high signal intensity sensitivity for the low concentrations of contrast agent expected to enter into rat hepatocytes.[28,29] However, with the sequence used, the range of contrast agent amount or concentration along which the signal intensity linearly increases is short, and the signal intensity rapidly saturates and even declines due to the growing importance of T2 effect. In clinical practice, such artifact may lead to erroneous image interpretation. Integration of a saturation equation in the model circumvented this difficulty.

Analyzing radioactivity and MRI data with a single pharmacokinetic model represents a real advantage when compared with our previous modeling of MRI data in normal rats with an individual approach,[15] in which the model developed from radioactivity data had to be reduced for MRI data, some rate constants being unidentifiable. The population approach also allows investigating different experimental conditions within a common framework, the interpretation of each experiment gaining strength from information accumulated from other experiments. The efficiency of the population approach to handle heterogeneous MRI data was previously underlined by several authors (eg, for the assessment of contrast agent kinetics in tumors).[17,18]

By modeling Gd-BOPTA transport in cirrhotic livers, we showed an increased extracellular distribution, associated with a decreased efflux to perfusate. A high extracellular distribution of Gd-BOPTA has been previously described in patients with cirrhosis.[2] Moreover, cirrhosis was associated with a decreased entry of Gd-BOPTA into hepatocytes, in agreement with the reduced expression of Oatp transporters in cirrhosis.[13,14] Gd-BOPTA efflux back to the extracellular space increased in BDL-1 but remained similar to normal in BDL-60 rats. This observation might be explained by an early increased expression of transporters located in the sinusoidal membrane that mediate the efflux of Gd-BOPTA back to the sinusoids. Such mechanism after acute bile duct ligation

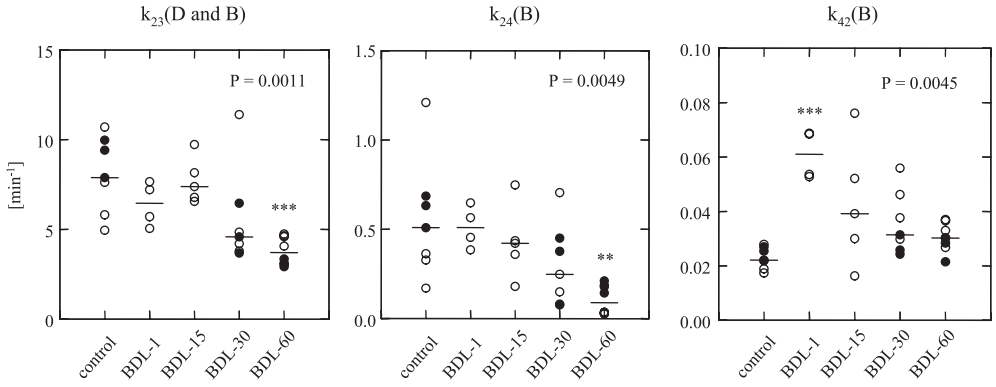

FIGURE 5. Pharmacokinetic parameters k_{23}(D and B), k_{24}(B) and k_{42}(B) in livers isolated from normal rats (n = 7), rats that had a bile duct ligation 1–2 hours before hepatic perfusion (BDL-1, n = 4), BDL-15 rats (n = 5), BDL-30 rats (n = 7), and BDL-60 rats (n = 8). The horizontal bar indicates the median, white symbols are MRI experiments, and black symbols are radioactivity experiments. *P* values refer to Kruskal–Wallis analysis and *to Dunn's multiple comparison test (**$P < 0.01$, ***$P < 0.001$).

© 2007 Lippincott Williams & Wilkins

Copyright © Lippincott Williams & Wilkins. Unauthorized reproduction of this article is prohibited.

might initially protect hepatocytes from high concentration of toxic compounds, such as bile acids that also enter into hepatocytes through Oatps. However, during chronic bile duct ligation (BDL-15, BDL-30, and BDL-60), Gd-BOPTA return back to the sinusoids remained within normal values. Although entry of contrast agent into hepatocytes was lower in cirrhotic than in normal livers, accumulation of Gd-BOPTA was higher in cirrhotic livers because biliary excretion was totally abolished. When livers were perfused with Gd-BOPTA and bromosulfophthalein (a pharmacological inhibitor of Oatps transporters), the signal intensity remained close to that obtained during Gd-DTPA perfusion. Pharmacokinetic modeling showed that Gd-BOPTA entry into hepatocytes was reduced 10 times by bromosulfophthalein, whereas other cellular processes were unaffected. Thus, bromosulfophthalein only interferes with Gd-BOPTA uptake.

In conclusion, the population pharmacokinetic approach developed in this study allows for quantification of Gd-BOPTA transport in livers measured by radioactivity and MRI. The model evidences that entry of Gd-BOPTA into hepatocytes is decreased in BDL-induced cirrhotic livers when compared with normal livers, although MR signal intensity is similar in normal and cirrhotic livers. Such a model-based approach might help to better interpret liver imaging with hepatobiliary contrast agents in patients with cirrhosis for whom controversial observations are reported, the signal intensity being either lower[30] or higher[2] than in healthy volunteers.

REFERENCES

1. Hamm B, Kirchin M, Pirovano G, et al. Clinical utility and safety of MultiHance in magnetic resonance imaging of liver cancer: results of multicenter studies in Europe and the USA. *J Comput Assist Tomogr*. 1999;23:S53–S60.
2. Manfredi R, Maresca G, Baron RL, et al. Gadobenate dimeglumine (BOPTA) enhanced MR imaging: patterns of enhancement in normal liver and cirrhosis. *J Magn Reson Imaging*. 1998;8:862–867.
3. Schneider G, Maas R, Kool SL, et al. Low-dose gadobenate dimeglumine versus standard dose gadopentetate dimeglumine for contrast-enhanced magnetic resonance imaging of the liver: an intra-individual crossover comparison. *Invest Radiol*. 2003;38:85–94.
4. Kuwatsuru R, Kadoya M, Ohtomo K, et al. Comparison of gadobenate dimeglumine with gadopentetate dimeglumine for magnetic resonance imaging of liver tumors. *Invest Radiol*. 2001;36:632–641.
5. Grazioli L, Morana G, Kirchin MA, et al. Accurate differentiation of focal nodular hyperplasia from hepatic adenoma at gadobenate dimeglumine-enhanced MR imaging: prospective study. *Radiology*. 2005; 236:166–177.
6. Clément O, Siauve N, Lewin M, et al. Contrast agents in magnetic resonance imaging of the liver: present and future. *Biomed Pharmacother*. 1998;52:51–58.
7. Hahn PF, Saini S. Liver-specific MR imaging contrast agents. *Radiol Clin North Am*. 1998;36:287–297.
8. Pastor CM, Planchamp C, Pochon S, et al. Kinetics of gadobenate dimeglumine in isolated perfused rat liver: MR imaging evaluation. *Radiology*. 2003;229:119–125.
9. Schuhmann-Giampieri G, Frenzel T, Schmitt-Willich H. Pharmacokinetics in rats, dogs and monkeys of a gadolinium chelate used as a liver-specific contrast agent for magnetic resonance imaging. *Drug Res*. 1993;43:927–931.
10. Lorusso V, Arbughi T, Tirone P, et al. Pharmacokinetics and tissue distribution in animals of gadobenate ion, the magnetic resonance imaging contrast enhancing component of gadobenate dimeglumine 0.5 M solution for injection (MultiHance). *J Comput Assist Tomogr*. 1999; 23:S181–S194.
11. Pascolo L, Petrovic S, Cupelli F, et al. ABC protein transport of MRI contrast agents in canalicular rat liver plasma vesicles and yeast vacuoles. *Biochem Biophys Res Commun*. 2001;282:60–66.
12. de Haën C, Lorusso V, Tirone P. Hepatic transport of gadobenate dimeglumine in TR-rats. *Acad Radiol*. 1996;3:S452–S454.
13. Dumont M, Jacquemin E, D'Hont C, et al. Expression of the liver Na^+-independent organic anion transporting polypeptide (oatp-1) in rats with bile duct ligation. *J Hepatol*. 1997;27:1051–1056.
14. Planchamp C, Montet X, Frossard J-L, et al. Magnetic resonance imaging with hepatospecific contrast agents in cirrhotic rat livers. *Invest Radiol*. 2005;40:187–194.
15. Planchamp C, Pastor CM, Balant L, et al. Quantification of Gd-BOPTA uptake and biliary excretion from dynamic MRI in rat livers: model validation with ^{153}Gd-BOPTA. *Invest Radiol*. 2005;40:705–714.
16. Aarons L. Population pharmacokinetics: theory and practice. *Br J Clin Pharmacol*. 1991;32:669–670.
17. Port RE, Knopp MV, Brix G. Dynamic contrast-enhanced MRI using Gd-DTPA: interindividual variability of the arterial input function and consequences for the assessment of kinetics in tumors. *Magn Reson Med*. 2001;45:1030–1038.
18. Spilker ME, Seng KY, Yao AA, et al. Mixture model approach to tumor classification based on pharmacokinetic measures of tumor permeability. *J Magn Reson Imaging*. 2005;22:549–558.
19. Planchamp C, Gex-Fabry M, Dornier C, et al. Gd-BOPTA transport into rat hepatocytes: pharmacokinetic analysis of magnetic resonance images using a hollow fiber bioreactor. *Invest Radiol*. 2004;39:506–515.
20. Port RE, Knopp MV, Hoffmann U, et al. Multicompartment analysis of gadolinium chelate kinetics: blood-tissue exchange in mammary tumors as monitored by dynamic MR imaging. *J Magn Reson Imaging*. 1999; 10:233–241.
21. Sheiner LB, Ludden TM. Population pharmacokinetics/dynamics. *Annu Rev Pharmacol Toxicol*. 1992;32:185–209.
22. Wagner JG. Integrated equations for several pharmacokinetic models. *Biopharmaceutics and Relevant Pharmacokinetics*. Halmilton, IL: Drug Intelligence Publications; 1971:292–296.
23. Cavagna FM, Maggioni F, Castelli PM, et al. Gadolinium chelates with weak binding to serum proteins. A new class of high-efficiency, general purpose contrast agents for magnetic resonance imaging. *Invest Radiol*. 1997;32:780–796.
24. de Haën C, Cabrini M, Akhnana L, et al. Gadobenate dimeglumine 0.5 M solution for injection (MultiHance): pharmaceutical formulation and physicochemical properties of a new magnetic resonance imaging contrast medium. *J Comput Assist Tomogr*. 1999;23:S161–S168.
25. Giesel FL, von Tengg-Kobligk H, Wilkinson ID, et al. Influence of human serum albumin on longitudinal and transverse relaxation rates (r1 and r2) of magnetic resonance contrast agents. *Invest Radiol*. 2006;41: 222–228.
26. Pintaske J, Martirosian P, Graf H, et al. Relaxivity of gadopentetate dimeglumine (magnevist), gadobutrol (gadovist), and gadobenate dimeglumine (multihance) in human blood plasma at 0.2, 1.5, and 3 Tesla. *Invest Radiol*. 2006;411:213–221.
27. Wersebe A, Wiskirchen J, Decker U, et al. Comparison of gadolinium-BOPTA and ferucarbotran-enhanced three-dimensional T1-weighted dynamic liver magnetic resonance imaging in the same patient. *Invest Radiol*. 2006;41:264–271.
28. Ivancevic MK, Zimine I, Lazeyras F, et al. FAST sequences optimization for contrast media pharmacokinetic quantification in tissue. *J Magn Reson Imaging*. 2001;14:771–778.
29. Vallée JP, Ivancevic M, Lazeyras F, et al. Use of high flip angle in T1-prepared FAST sequences for myocardial perfusion quantification. *Eur Radiol*. 2003;13:507–514.
30. Grazioli L, Morana G, Caudana R, et al. Hepatocellular carcinoma: correlation between gadobenate dimeglumine-enhanced MRI and pathologic findings. *Invest Radiol*. 2000;35:25–34.

© 2007 Lippincott Williams & Wilkins

Copyright © Lippincott Williams & Wilkins. Unauthorized reproduction of this article is prohibited.